

EFFECTS OF THERMAL RADIATION, JOULE HEATING AND POROUS MEDIUM ON THE FLOW OF A THIN LIQUID FILM ON AN UNSTEADY STRETCHING SHEET

R.S. Yadav¹ and O.D. Makinde²

¹Department of Mathematics, University of Rajasthan, Jaipur, India

²Faculty of Military Science, Stellenbosch University, South Africa

Email: rajendraur@gmail.com, makinded@gmail.com

Abstract: Numerical analysis of MHD flow and heat transmission in a thin liquid film over an impermeable stretching sheet is investigated. Similarity transformations are used to handle the governing time-dependent nonlinear boundary layer equations. The boundary value problem is solved by an efficient shooting algorithm with fourth order Runge-Kutta technique. The effects of physical parameters on the fluid velocity and heat transfer are shown through graphs and analyzed. Skin friction coefficient and Nusselt number at the sheet are analyzed numerically.

Keywords: Viscous fluid, MHD, Thermal radiation, Porous medium.

1. Introduction

Study of boundary layer flow on thin liquid film has encountered enormous involvement from researches for the past decades because of its possible applications in industry and technology. An understanding of flow and heat transfer within a thin liquid film is important in considering design of various heat exchangers, fiber coating processes, drawing of a polymer sheet, tinning of copper wires and aerodynamic extrusion of plastic sheets. Such application involve cooling of a liquefied by drawing it into a cooling system. In drawing the molten liquid into the cooling system, it is quondam stretched as in the case of polymer extrusion process. The fiber coating process requires a smooth surface for the best product appearance and for such properties as low friction and strength. Therefore the analysis of flow and heat transfer within thin liquid film on a stretching sheet is important for understanding some fundamentals of such extrusion processes. Crane [6] observed flow past a stretching plane. Grubka and Bobba [13] studied heat transfer characteristics of a continuous stretching surface with variable temperature. Dutta and Gupta [11] studied cooling of a stretching sheet in a various flow. Wang [22] considered stretching a surface in a rotating fluid. Usha and Sridharan [22] considered the axisymmetric motion of a liquid film on an unsteady stretching surface. Andersson et al. [3] studied heat transfer in a liquid film on an unsteady stretching surface. Muralidhar and Sundarajan [18] studied computational fluid flow and heat transfer. Dandapat et al. [7] obtained thermocapillarity in

a liquid film on an unsteady stretching sheet. Cortell [5] considered viscoelastic fluid flow and heat transfer over a stretching sheet under the effects of a non-uniform heat source, viscous dissipation and thermal radiation. Dandapat et al. [8] presented effects of variable fluid properties and thermocapillarity on the flow of a thin film on an unsteady stretching sheet. Abel, Mahesha and Tawade [1] discussed heat transfer in a liquid film over an unsteady stretching surface with viscous dissipation in presence of external magnetic field. Sharma and Singh [21] investigated effects of varying viscosity and thermal conductivity on steady MHD free convective flow and heat transfer along an isothermal plate with internal heat generation. Noor and Hashim [20] considered thermo capillarity and magnetic field effects in a thin liquid film on an unsteady stretching surface. Hydromagnetic flow and heat transfer with thermal radiation effects have been discussed by Eegunjobi and Makinde [12], Ibrahim and Makinde ([14], [15]), Das et al. ([9], [10]) and Ali et al. [2]. In above studies, the combined effect of Joule heating and the thermal emission on the flow of a thin liquid film over an unsteady stretching sheet enclosed in a porous medium was not considered. Aim of the paper is to investigate the MHD flow and heat transfer in a thin liquid film on an unsteady stretching sheet under the following assumptions:

- a. The sheet is expanded by the act of an identical force along the x-axis.
- b. The effect of latent hotness due to evaporation has ignored as liquid to be nonvolatile.
- c. The elastic sheet is extremely larger than the thin liquid film so buoyancy force is ignored.
- d. The liquid film is not so small that intermolecular forces appear within consideration.
- e. The pressure is homogenous in the neighboring gas phase and the gravity force provides boost to a hydrostatic pressure variation in the thin liquid film.
- f. Height of the film thickness is taken as $(\nu/b)^{1/2}$ so that the ratio is suitable i.e.

$$\frac{x}{(\nu/b)^{1/2}} \approx 1.$$

2. Mathematical Formulation

Consider two dimensional flow of a viscous, incompressible fluid over impermeable stretching sheet which materialize from a definite slot at the origin of the coordinate system. The uninterrupted sheet at $y=0$ is parallel with the x-axis and moves with the velocity

$$U(x,t) = \frac{bx}{(1-at)}, \quad (1)$$

where a and b are absolute constants with entity $(\text{time})^{-1}$. Expression (1) for the velocity of the sheet $U(x, t)$ shows that the elastic surface is expanded by yielding a force in the positive x-direction and the factual stretching rate $b/(1-at)$ rise with time as $0 \leq a < 1$. The surface temperature T_s of the sheet is considered to fluctuate with the distance x from the slot as

$$T_s(x,t) = T_0 - T_{ref} \left[bx^2 / 2\nu \right] (1-at)^{-3/2}, \quad (2)$$

where T_0 is the temperature at the slot and T_{ref} is the constant reference temperature such that $0 \leq T_{ref} \leq T_0$.

The term $bx^2 / \nu(1-at)$ can be acknowledged as the local Reynolds number.

Expression (2) shows that the amount of temperature dimension along the sheet increases with time. Consider a thin elastic liquid film of uniform thickness $h(t)$ lies on the horizontal sheet. The x-axis is taken in the direction along which the sheet is determined to move and the y-axis is taken perpendicular to it.

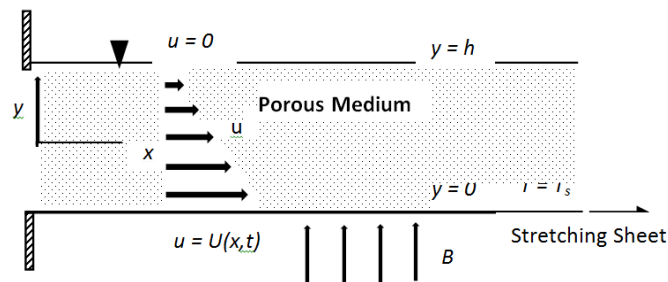


Figure 1. Systematic sketch of demonstrated problem.

The continuous moving horizontal stretching sheet embedded in a porous medium and influenced by an external transverse magnetic field of strength B_0 as shown in figure 1. In view of the above, the governing equations of continuity, momentum and energy (Refs. [4], [7] and [19]) are given by

$$\frac{\partial u}{\partial x} + \frac{\partial v}{\partial y} = 0, \quad (3)$$

$$\frac{\partial u}{\partial t} + u \frac{\partial u}{\partial x} + v \frac{\partial u}{\partial y} = \nu \frac{\partial^2 u}{\partial y^2} - \frac{\sigma B^2}{\rho} u - \frac{\nu}{k} u, \quad (4)$$

$$\frac{\partial T}{\partial t} + u \frac{\partial T}{\partial x} + v \frac{\partial T}{\partial y} = \frac{\kappa}{\rho C_p} \frac{\partial^2 T}{\partial y^2} + \frac{\nu}{C_p} \left(\frac{\partial u}{\partial y} \right)^2 + \frac{\sigma B^2 u^2}{\rho C_p} + \frac{\nu u^2}{C_p k} - \frac{1}{\rho C_p} \frac{\partial q_r}{\partial y}, \quad (5)$$

where u and v are velocity components along the x and y directions, respectively; $\nu (= \mu / \rho)$ is the kinematic viscosity, μ is the coefficient of viscosity, σ is the electrical conductivity, ρ is the density of the fluid, k is the permeability of the porous medium, T is fluid temperature inside the thermal boundary layer, T_∞ is the fluid temperature in the free stream, κ is the thermal conductivity and C_p is the specific heat at constant pressure, q_r is the radioactive heat flux.

Following Rosseland's approximation, the radioactive heat flux q_r is modeled as

$$q_r = -\frac{4\sigma^*}{3k^*} \frac{\partial T^4}{\partial y}, \quad (6)$$

where σ^* is the Stefan-Boltzman constant, k^* is the mean absorption coefficient. Assuming so that the temperature variation within the flow is suitably limited such that T^4 may be shown as a linear function of temperature $T^4 \equiv 4T_0^3 T - 3T_0^4$, we have

$$\frac{\partial q_r}{\partial y} = -\frac{16\sigma^* T_0^3}{3k^*} \frac{\partial^2 T}{\partial y^2}. \quad (7)$$

The boundary conditions are given by

$$y = 0: u = U(x, t), \quad v = 0, \quad T = T_s(x, t), \quad (8)$$

$$y \rightarrow h: \frac{\partial u}{\partial y} = \frac{\partial T}{\partial y} = 0, \quad (9)$$

$$y \rightarrow h: v = \frac{dh}{dt}, \quad (10)$$

where h is the thickness of thin liquid film and $T_s(x, t)$ is the temperature of the sheet.

3. Solution of the problem

Introducing the following similarity variable and dimensionless functions

$$\eta = (b/\nu)^{1/2} (1-at)^{-1/2} y, \quad (11)$$

$$f(\eta) = \Psi(x, y, t) \left[\nu b x^2 / (1-at) \right]^{-1/2}, \quad (12)$$

$$\theta(\eta) = \frac{(T_0 - T)}{T_{ref}} \left(\frac{2\nu}{bx^2} \right) (1-at)^{3/2}, \quad (13)$$

$$u = \frac{\partial \Psi}{\partial y} = bx(1-at)^{-1} f'(\eta), \quad (14)$$

$$v = -\frac{\partial \Psi}{\partial x} = -(\nu b)^{1/2} (1-at)^{-1/2} f(\eta). \quad (15)$$

Into the equations (5) and (6), we get

$$f'''' - (M + D + S)f' = (S\eta/2) f'' + (f')^2 - ff'', \quad (16)$$

$$(1 + Nr)\theta'' = \frac{\text{Pr}}{2} [S(3\theta + \eta\theta')] + \text{Pr}(2f'\theta - f\theta') - Ec \text{Pr}(f'')^2 - (M + D)Ec \text{Pr}(f')^2, \quad (17)$$

where prime indicates differentiation with respect to η , $S(= a/b)$ is the dimensionless measure of the unsteadiness, $M \left(= \frac{\sigma B_0^2}{\rho b} \right)$ is the magnetic parameter, $D \left(= \frac{\nu(1-at)}{bk} \right)$ is the

Darcy number, $\text{Pr} \left(= \frac{\mu C_p}{\kappa} \right)$ is the Prandtl number, $Nr \left(= \frac{16\sigma^* T_0^3}{3\kappa k^*} \right)$ is the radiation parameter, $Ec \left(= \frac{U^2}{C_p(T_s - T_0)} \right)$ is the Eckert number and $\beta \left(= h(b/\nu)^{1/2} (1-at)^{-1/2} \right)$

expresses the value of the similarity variable η at the free surface.

It is observed that the equation of continuity (4) is identically satisfied. Now, the boundary conditions are reduced to

$$f(0) = 0, f'(0) = 1, \theta(0) = 1, f(\beta) = S\beta/2, f''(\beta) \rightarrow 0, \theta'(\beta) \rightarrow 0 \quad (18)$$

4. Skin friction Coefficient

The skin friction coefficient at the surface is defined as

$$C_f = \frac{2\tau_w}{\rho U^2} \quad (19)$$

$$\Rightarrow C_f = -2\text{Re}^{-1/2} f''(0), \quad (20)$$

where $\tau_w \left(= -\mu \left(\frac{\partial u}{\partial y} \right)_{y=0} \right)$ is the shearing stress at the surface and $\text{Re} \left(= \frac{xU}{\nu} \right)$ is the Reynolds number.

5. Heat transfer Coefficient

The rate of heat transfer in terms of Nusselt number at the surface is given by

$$Nu_x = \frac{x}{\kappa T_{ref}} (q_w + q_r), \quad (21)$$

$$\Rightarrow Nu_x = \frac{1}{2} (1 + Nr) (1 - at)^{-1/2} \text{Re}^{3/2} \theta'(0) \quad (22)$$

where $q_w \left(= -\kappa \left(\frac{\partial T}{\partial y} \right)_{y=0} \right)$ is the rate of heat transfer at the surface.

6. Numerical Method

Equations (17) and (18) are non-linear ordinary coupled differential equations and solved using an efficient shooting approach with fourth order Runge-Kutta integration technique (Refs. [16] and [17]). The non-linear equations are converted into a sequence of first order differential equations. In this process, f_1, f_2, f_3, f_4 and f_5 are used instead of f, f', f'', θ and θ' , respectively as given by

$$f_1' = f_2, \tag{23}$$

$$f_2' = f_3, \tag{24}$$

$$f_3' = (M + D + S)f_2 - f_1f_3 + f_2^2 + \frac{1}{2}S\eta f_3, \tag{25}$$

$$f_4' = f_5, \tag{26}$$

$$f_5' = \frac{Pr}{(1 + Nr)} \left[\frac{S}{2} (3f_4 + \eta f_5) + 2f_2f_4 - f_1f_5 - Ec f_3^2 - (M + D) Ec f_2^2 \right]. \tag{27}$$

Subsequently, the boundary conditions (19) are reduced to

$$f_1(0) = 0, f_2(0) = 1, f_4(0) = 1, f_3(\beta) \rightarrow 0, f_5(\beta) \rightarrow 0, f_1(\beta) = \frac{S\beta}{2}. \tag{28}$$

The resolved first order differential equations with boundary conditions are now converted into an initial value problem by suitable suppositions of the unknown values $f_3(0)$ and $f_5(0)$. The value of β is taken so that the situation $f_1(\beta) = \frac{S\beta}{2}$ controls. The convergence standards are based on the best shots of the unknown initial values $f_3(0)$ and $f_5(0)$.

7. Results and Discussion

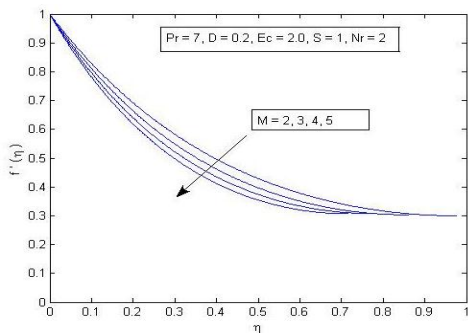


Figure 2. Velocity profiles versus η (effect of magnetic parameter).

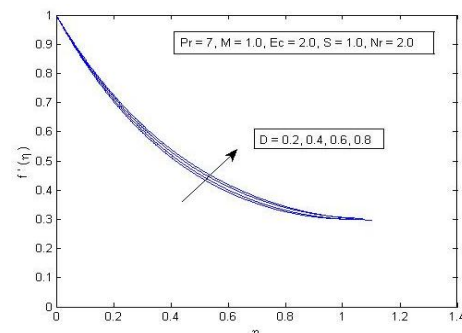


Figure 3. Velocity profiles versus η (effect of Darcy number).

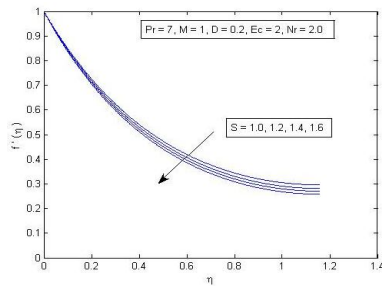


Figure 4. Velocity profiles versus η (effect of unsteadiness parameter).

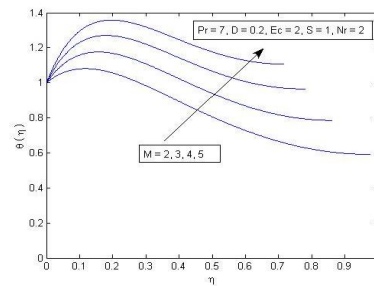


Figure 5. Temperature profiles versus η (effect of magnetic parameter).

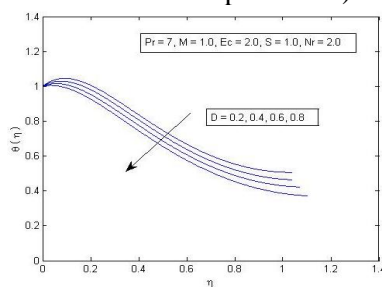


Figure 6. Temperature profiles versus η (effect of Darcy number).

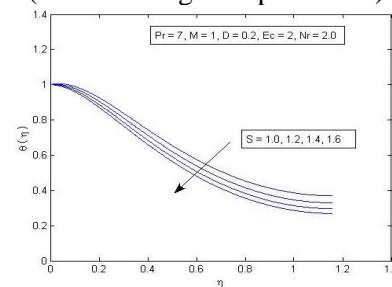


Figure 7. Temperature profiles versus η (effect of unsteadiness parameter).

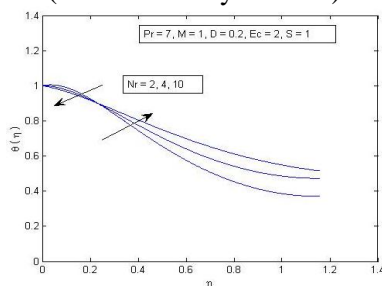


Figure 8. Temperature profiles versus η (effect of radiation parameter).

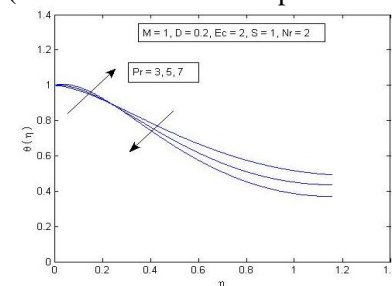


Figure 9. Temperature profiles versus η (effect of Prandtl number).

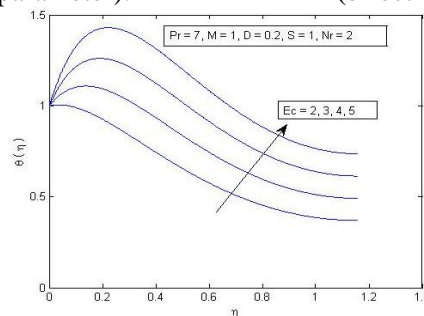


Figure 10. Temperature profiles versus η (effect of Eckert number).

It is noted from figure 2 that due to increase in magnetic parameter, the velocity of fluid decreases. Application of a transverse magnetic field results in a drag force called the Lorentz force. This force tends to slow down the movement of the fluid along surface. Hence it decreases magnitude of velocity of fluid in thin liquid film.

It is revealed from figure 3 that the velocity rises with the increase of Darcy number. Physically, this is due to the fact that increase in the value of Darcy number leads to drop permeability of the porous media. It is observed from figure 4 that fluid velocity decreases with the distance from the stretching sheet for all values of unsteadiness parameter. Also increasing the values of unsteadiness parameter, it decreases the velocity profile in the boundary layer.

It is noted from figure 5 that the thermal boundary layer width rises with the increasing value of magnetic parameter. The frictional drag due to the Lorentz force is responsible for rising in the thermal boundary layer width. This force opposes the fluid motion. Due to this heat is produced and the thermal boundary layer width increases.

It is obvious from figure 6 that the increase of the Darcy number leads to decrease in the fluid temperature. Physically, greater Darcy number implies smaller permeability of porous medium. This corresponds to decrease in thermal conduction heat transfer within the medium. Figure 7 depicts that temperature of the fluid decreases with the distance from the stretching sheet for all values of unsteadiness parameter. Also increasing the values of unsteadiness parameter, it decreases the temperature profile in the thermal boundary layer.

Figure 8 demonstrates that near the stagnation point the temperature decreases but far away from the stagnation point the temperature increases with the increase in radiation parameter. This is true because the Rosseland's approximation results an increase in temperature profile.

Figure 9 illustrates that far away from the stagnation point the temperature decreases with increase in Prandtl number. Prandtl number signifies the ratio of momentum to thermal diffusivity. Larger values of Prandtl number has momentum diffusivity higher than the thermal diffusivity and hence temperature profile decreases with increase in Prandtl number.

It is noted from figure 10 that fluid temperature increases with the increase in Eckert number. Eckert number expresses the conversion of kinetic energy into internal energy. Viscous dissipation creates heat due to resistance between fluid particles, which leads rise in fluid temperature. That is, an increase in the magnitude of Eckert number contributes to the thickening of the thermal boundary layer.

The effect of joule heating parameter is characterized by the product of magnetic parameter and Eckert number. It is illustrated from figure 5 and figure 10 that temperature increases with increase in the value of Joule heating parameter. Due to internal friction of molecules of the fluid, the mechanical energy converted into thermal energy is responsible for temperature increment.

In order to validate the numerical technique used and to judge the certainty of the present analysis, the numerical values of skin friction coefficient and Nusselt number are

compared with those of carried out by Abel et al. (2009) and shown through Tables 1 and 2. A good agreement is observed between these results. This extends assurance in the numerical results to be reported subsequently.

Also, the numerical data for various values of physical parameters are derived according to the physical phenomena of parameters. It is observed from table 3 that as the Darcy number rises, the values of the skin friction coefficient and Nusselt number increased. It is noted that the skin friction coefficient raises, but the Nusselt number declines with the rise of unsteadiness parameter. It is seen that Nusselt number decreased with the increase of radiation parameter. However, due to increase in Prandtl number or Eckert number, it is found that the Nusselt number increases. It is discovered that as the Darcy number rises, the values of the skin friction coefficient and Nusselt number increased.

Table 1 Comparison of numerical values of $f''(0)$ for various values of λ for thin liquid film when $M = 0$ and $K = 0$.

| S | Abel et al. (2009) | | Present study | |
|-----|--------------------|-----------|---------------|-----------|
| | β | $f''(0)$ | β | $f''(0)$ |
| 0.4 | 4.981455 | -1.134098 | 4.981445 | -1.134087 |
| 0.6 | 3.131710 | -1.195128 | 3.132286 | -1.195097 |
| 0.8 | 2.151990 | -1.245805 | 2.151992 | -1.245831 |
| 1.0 | 1.543617 | -1.277769 | 1.543635 | -1.277780 |
| 1.2 | 1.127780 | -1.279171 | 1.127779 | -1.279352 |
| 1.4 | 0.821033 | -1.233545 | 0.821033 | -1.233610 |
| 1.6 | 0.576176 | -1.114941 | 0.576173 | -1.114944 |
| 1.8 | 0.356390 | -0.867416 | 0.356390 | -0.867416 |

Table 2 Comparison of numerical values of $\theta'(0)$ for various values of Pr when $M = 0, K = 0, Nr = 0$ and $Ec = 0$.

| Pr | Abel et al. (2009) $\theta'(0)$ | Present study $\theta'(0)$ | Present study $f''(0)$ |
|---------------------------------|------------------------------------|-------------------------------|---------------------------|
| $S = 0.8$ and $\beta = 2.15199$ | | | |
| 0.1 | -0.351920 | -0.340040 | -1.248320 |
| 1 | -1.671919 | -1.671089 | -1.248320 |
| 2 | -2.443914 | -2.442501 | -1.248320 |

| | | | |
|------------------------------|-----------|-----------|-----------|
| 3 | -3.034915 | -3.034978 | -1.248320 |
| $S=1.2$ and $\beta=1.127780$ | | | |
| 0.1 | -0.305409 | -0.305206 | -1.217907 |
| 1 | -1.773772 | -1.773432 | -1.217907 |
| 2 | -2.638431 | -2.638245 | -1.217907 |
| 3 | -3.280329 | -3.280415 | -1.217907 |

Table 3 Numerical values of skin friction coefficient and Nusselt number at the surface of the sheet for various values of physical parameters.

| M | S | Nr | Pr | Ec | D | β | $-f''(0)$ | $\theta'(0)$ |
|-----|-----|------|------|------|-----|---------|-----------|---------------|
| 1 | 1 | 2 | 7 | 2 | 0.2 | 1.1560 | 1.653368 | 0.321924 |
| 2 | 1 | 2 | 7 | 2 | 0.2 | 0.97602 | 1.90742 | 1.579650 |
| 3 | 1 | 2 | 7 | 2 | 0.2 | 0.8616 | 2.13059 | 2.724501 |
| 4 | 1 | 2 | 7 | 2 | 0.2 | 0.78002 | 2.3306 | 3.93987 |
| 1 | 1.2 | 2 | 7 | 2 | 0.2 | 1.1560 | 1.70575 | 0.214074 |
| 1 | 1.4 | 2 | 7 | 2 | 0.2 | 1.1560 | 1.75503 | 0.112806 |
| 1 | 1.6 | 2 | 7 | 2 | 0.2 | 1.1560 | 1.8035 | 0.023111 |
| 1 | 1 | 4 | 7 | 2 | 0.2 | 1.1560 | 1.653368 | 0.020805 |
| 1 | 1 | 8 | 7 | 2 | 0.2 | 1.1560 | 1.653368 | - 0.121301 |
| 1 | 1 | 10 | 7 | 2 | 0.2 | 1.1560 | 1.653368 | -0.14009 |
| 1 | 1 | 2 | 5 | 2 | 0.2 | 1.1560 | 1.653368 | 0.101010 |
| 1 | 1 | 2 | 3 | 2 | 0.2 | 1.1560 | 1.653368 | - 0.081023 |
| 1 | 1 | 2 | 1 | 2 | 0.2 | 1.1560 | 1.653368 | -0.13304 |
| 1 | 1 | 2 | 7 | 3 | 0.2 | 1.1560 | 1.653368 | 1.83350 |
| 1 | 1 | 2 | 7 | 4 | 0.2 | 1.1560 | 1.653368 | 3.34534 |
| 1 | 1 | 2 | 7 | 5 | 0.2 | 1.1560 | 1.653368 | 4.85730 |
| 1 | 1 | 2 | 7 | 2 | 0.4 | 1.10042 | 1.70440 | 0.576520 |
| 1 | 1 | 2 | 7 | 2 | 0.6 | 1.07002 | 1.75906 | 0.84002 |
| 1 | 1 | 2 | 7 | 2 | 0.8 | 1.03602 | 1.80934 | 1.08925 |

8. Conclusions

In the present study the effect of magnetic field and the thermal radiation on the flow of a thin liquid film over an unsteady stretching sheet embedded in a porous medium is investigated. Some of the influential findings are given below:

1. It is observed that as unsteadiness parameter increases the velocity of fluid flow in thin liquid film decreases.
2. The velocity of fluid flow in thin liquid film decreases with the increase of magnetic parameter.
3. Thermal boundary layer thickness enlarges with the hike of magnetic parameter.
4. The rise of the radiation parameter leads to decrease in the temperature of the fluid near the stagnation point but it increases far away from the sheet.
5. Fluid temperature in thin liquid film decreases with rise in Darcy Number.
6. Temperature of the fluid rises with the increase of Eckert Number.
7. Skin friction coefficient at the surface of sheet increases with an increase in unsteadiness parameter, while Nusslet number decreases with an increase in unsteadiness parameter.
8. Nusselt number rises with the rise of Prandtl number, while it decreases due to rise of radiation parameter.
9. Skin friction coefficient and Nusselt number both increase with the increase of magnetic parameter or Darcy number.

Acknowledgement

The authors dedicate gratitude towards Late Prof. P. R. Sharma for extended discussions and valuable suggestions which have contributed greatly towards finalization of the paper. The authors are extremely thankful to the anonymous referee for the fruitful comments given for the improvement of the present paper,

References

- [1] Abel, M.S., Mahesha, N. and Tawade, J. (2009). Heat transfer in a liquid film over an unsteady stretching surface with viscous dissipation in presence of external magnetic field, *Applied Mathematical Modelling*, **33**, 3430-3441.
- [2] Ali, A.O., Makinde O. D. and Nkansah-Gyekye Y. (2016). Numerical study of unsteady MHD Couette flow and heat transfer of nanofluids in a rotating system with convective cooling, *International Journal of Numerical Methods for Heat & Fluid Flow*, **26** (5), 1567-1579.
- [3] Andersson, H. I., Aarseth, J. B. and Dandapat, B. S. (2000). Heat transfer in a liquid film on an unsteady stretching surface, *Int. J. Heat and Mass Transfer*, **43**, 69-74.

- [4] Bansal, J. L. (1997). *Viscous Fluid Dynamic*,. Oxford & IBH Pub. Co., New Delhi, India.
- [5] Cortell, R. (2007). Viscoelastic fluid flow and heat transfer over a stretching sheet under the effects of a non-uniform heat source, viscous dissipation and thermal radiation, *Int. J. Heat and Mass Transfer*, **50**, 3152–3162.
- [6] Crane, L. J. (1970). Flow past a stretching plane, *Z. Angew. Math. Phys.* **21**, 645-647.
- [7] Dandapat, B. S., Santra, B. and Andersson, H. I. (2003). Thermocapillarity in a liquid film on an unsteady stretching sheet, *Int. J. Heat and Mass Transfer*, **46**, 3009-3015.
- [8] Dandapat, B. S., Santra, B. and Vajravelu, K. (2007). The effects of variable fluid properties and thermocapillarity on the flow of a thin film on an unsteady stretching sheet, *Int. J. Heat and Mass Transfer*, **50**, 991–996.
- [9] Das, S., Jana, R.N. and Makinde, O.D. (2016a). Transient hydromagnetic reactive Couette flow and heat transfer in a rotating frame of reference, *Alexandria Engineering Journal*, **55**(1), 635-644.
- [10] Das, S., Jana, R.N. and Makinde, O.D. (2016b). Magnetohydrodynamic free convective flow of nanofluid past an oscillating porous flat plate in a rotating system with thermal radiation and Hall effects, *Journal of Mechanics*, **32** (2), 197-210.
- [11] Dutta, B. K. and Gupta, A. S. (1987). Cooling of a stretching sheet in a various flow, *Ind. Eng. Chem. Res.*, **26**, 333–336.
- [12] Eegunjobi, A.S. and Makinde, O. D. (2015). Second law analysis for MHD permeable channel flow with variable electrical conductivity and asymmetric Navier slips. *Open Physics*, **13**, 100-110.
- [13] Grubka, L. G. and Bobba, K. M. (1985). Heat transfer characteristics of a continuous stretching surface with variable temperature, *J. Heat Trans.*, **107**, 248-250.
- [14] Ibrahim, W. and Makinde, O.D. (2016a). Magnetohydrodynamic stagnation point flow and heat transfer of Casson nanofluid past a stretching sheet with slip and convective boundary condition. *Journal of Aerospace Engineering*, **29** (2), Article number 04015037.
- [15] Ibrahim, W. and Makinde, O. D. (2016b). Magnetohydrodynamic stagnation point flow of a power-law nanofluid towards a convectively heated stretching sheet with slip, *Proceedings of the Institution of Mechanical Engineers, Part E: Journal of Process Mechanical Engineering*, **230** (5), 345-354.
- [16] Jain, M. K. (2000). *Numerical Solution of Differential Equations* New Age Int. Pub., New Delhi, India.

- [17] Jain, M. K., Iyengar, S. R. and Jain, R. K. (1985). *Numerical Methods for Scientific and Engineering Computation*, Wiley Eastern Ltd., New Delhi, India.
- [18] Muralidhar K. and Sundararajan, T. (2003). *Computational Fluid Flow and Heat Transfer*, Narosa Pub. House, New Delhi, India.
- [19] Nield, D. A. and Bejan, A. (2006). *Convection in Porous Media*, Springer, New York.
- [20] Noor, N.F.M. and Hashim, I. (2010). Thermocapillarity and magnetic field effects in a thin liquid film on an unsteady stretching surface, *Int. J. Heat and Mass Transfer*, **53**, 2044–2051.
- [21] Sharma, P.R. and Singh, G. (2009). Effects of varying viscosity and thermal conductivity on steady MHD free convective flow and heat transfer along an isothermal plate with internal heat generation, *Int. J. Num. Methods Heat Fluid Flow*, **19** (1), 78–92.
- [22] Usha, R. and Sridharan, R. (1995). The axisymmetric motion of a liquid film on an unsteady stretching surface, *ASME Journal of Fluids Eng.*, **117**, 81–85.
- [23] Wang, C.Y. (1988). Stretching a surface in a rotating fluid, *J. Appl. Math. Phys. (ZAMP)*, **39**, 177-185.

